이학박사 학위논문

세포괴사 조절 인자로서 카제인 키나아제 1 감마에 대한 연구

A study on the essential role of casein kinase gamma 1 and 3 in necroptosis

2018년 6월

서울대학교 대학원

생명과학부

이 송 이

A study on the essential role of casein kinase gamma 1 and 3 in necroptosis

Song-Yi Lee

Department of Biological Sciences

The Graduate School

Seoul National University

ABSTRACT

Upon necroptosis activation, receptor interacting serine/threonine kinase (RIPK) 1 and RIPK3 form a necrosome complex with pseudokinase mixed lineage kinase-like (MLKL). Although protein phosphorylation is a key event for the activation of RIPK1 and RIPK3 in response to necroptosis

signal, relatively little is known about other factors that can regulate the activity of those kinases or necrosome formation. In a gain-of-function screen with 650 kinases and 120 phosphatases, I identified that casein kinase 1 gamma (CK1γ) as a crucial regulator of necroptosis. Here I show that the downregulation of CK1γ1 and CK1γ3, either by a chemical inhibitor or knockdown in cells, reduced TNFα-induced necroptosis. Conversely, ectopic expression of CK1γ1 or CK1γ3 exacerbated necroptosis, but not apoptosis. Like RIPK1 and RIPK3, CK1γ1 was cleaved at Asp434 by caspase-8 during apoptosis, while it was increased in response to necroptosis. CK1γ1 and CK1γ3 formed a protein complex with each other and were recruited into the necrosome harboring RIPK1, RIPK3 and MLKL. Especially, autophosphorylated form of CK1γ3 at Ser344/345 was detected in the necrosome and was required to mediate the necroptosis. In addition, CK1γ phosphorylates RIPK3 *in vitro* and a CK1γ-specific inhibitor Gi reduced the phosphorylation of MLKL at Ser358, as well as

the formation of MLKL oligomers, and rescued mice from TNFα-induced systemic inflammatory response syndrome (SIRS). Collectively, these data suggest that CK1γ1 and CK1γ3 are required for promoting cell death progression by regulating the formation of necrosome through RIPK3.

Keywords : Necroptosis, casein kinases, RIPK3, screening, TNFα

Student number : 2012-30889

CONTENTS

LIST OF FIGURES

LIST OF TABLES

ABBREVIATIONS

CK	**Casein kinase**
DMEM	**Dulbecco's modified Eagle's medium**
DMSO	**Dimethyl sulfoxide**
FBS	**Fetal bovine serum**
GFP	**Green fluorescence protein**
GOF	**Gain-of-function**
GST	**Glutathione**
LOF	**Loss-of-function**
MLKL	**Mixed lineage kinase-like**
MS	**Mass spectrometry**
NAC	**N-acetyl-L-cysteine**
Nec1	**Necrostatin-1**
NSA	**Necrosulfonamide**
RIPK	**Receptor interacting serine/threonine kinase**

ROS	**Reactive oxygen species**
SIRS	**Systemic inflammatory response syndrome**
SM-164	**Smac mimetic-164**
TNFα	**Tumor necrosis factor alpha**
TRAIL	**TNF-related apoptosis-inducing ligand**

1. INTRODUCTION

Necroptosis is an important necrotic cell death mechanism that can mediate cell death under apoptosis-deficient conditions (Christofferson DE, Yuan J, 2010; Oberst A, et al., 2011; Kaiser WJ, et al., 2011; Zhang H, et al., 2011). Necroptosis is involved in many pathological conditions, such as sterile inflammation (He S, et al., 2009; Linkermann A, et al., 2013), neurodegenerative diseases and aborting defective embryos during embryonic development (Dillon CP, et al., 2014; Shan B, et al., 2018). The receptor interacting serine/threonine kinase (RIPK)1 and RIPK3 were identified as two decisive serine/threonine kinases mediating necroptosis. Inactivation of caspase-8 is a prerequisite for their activation, because caspase-8 cleaves and inactivates RIPK1 and RIPK3 by proteolytic cleavage (Lin Y, et al., 1999; Feng S, et al., 2007). Once this cleavage is prevented by either an inhibitor or genetic deletion of caspase-8, RIPK1 and RIPK3 can be activated through phosphorylation to form necroptosis-initiating complex with pseudokinase mixed lineage kinase-like (MLKL), referred to necrosome (Declercq W, et al., 2009; Murphy M, Silke J, 2014).

Upon necroptosis, posttranslational modifications play a key role. Besides aforementioned modifications like phosphorylation and caspase-mediated cleavage, the ubiquitination is also deeply engaged in necrosome formation. A20 is known to polyubiquitinate RIPK1 with K48-linked ubiquitin chains, thereby targeting RIPK1 for proteasomal degradation (Wertz IE, et al., 2004) or ubiquitinate RIPK3 at K5, which disturbs RIPK1-RIPK3 complex formation (Onizawa M, et al., 2015). Also, a RIPK1 K63-deubiquitinating enzyme, cylindromatosis (CYLD), allows RIPK1 to be released from the receptor and primed to form a cell death-initiating complex in cytosol (Wang X, et al., 2008).

Nonetheless, among these modifications, protein phosphorylation is considered to play the most essential role in regulating TNF-induced necroptosis (Murphy J, Vince J, 2015; Liu X, et al., 2016). The activation of RIPK1, RIPK3 and MLKL is marked by their phosphorylation (Rodriguez DA, et al., 2016) and multiple serine/threonine residues in these proteins are phosphorylated, which may be positively or negatively regulate their activities in case of RIPK1 and RIPK3 (Degterev A, et al., 2008; Chen W, et al., 2013; Geng J, et al., 2017). Among them,

phosphorylation of S166 is a biomarker of RIPK1 activation (Degterev A, et al., 2008, Ofengeim D, et al., 2015) and RIP3 Ser227 phosphorylation is needed for the recruitment and activation of MLKL (Sun L, et al., 2012). Recently, some kinases and phosphatases, other than RIPK1 and RIPK3 themselves, were reported to regulate the phosphorylation of RIP kinases. MAPK-activated protein kinase 2 (MK2) can directly phosphorylate RIPK1 and inhibit its activity (Dondelinger Y, et al., 2017; Jaco I, et al., 2017). In addition, protein phosphatase 1B (Ppm1b) is a phosphatase identified as a negative regulator to suppress necroptosis by dephosphorylating RIPK3 (Chen W, et al., 2015).

Casein kinase (CK)1γ is an isoform of CK1 family of serine/threonine kinases. Seven CK1 isoforms (α, β, γ1, γ2, γ3, δ and ε) and several splice variants have been found in vertebrates (Schittek B, Sinnberg T, 2014). All the isoforms share a highly conserved N-terminal kinase domain and a distinguished C-terminal domain. The C-terminal domain of CK1 isoforms gives each isoform a characteristic that regulates the substrate specificity and kinase activity. Even though many substrates have been identified to be phosphorylated by CK1 family

and regulate various cellular processes, such as Wnt signaling, cell cycle control, DNA repair apoptosis and circadian rhythms (Cheong J, Virshup D, 2011), little is known about the role of CK1γs in the regulation of necroptosis.

To discover regulator(s) involved in the phosphorylation-mediated regulation of necroptosis, I carried out a gain-of-functional (GOF) screen using cDNA expression library encoding 650 kinases and 120 phosphatases. Here I show that CK1γ1 and CK1γ3 are recruited into necrosome in response to necroptosis and exacerbate TNFα-induced necroptosis both *in vitro* and *in vivo*.

2. MATERIAL AND METHOD

2.1. Collection of cDNAs and GOF screening

The cDNAs encoding 650 protein kinases and 120 phosphatases were generated from subcloning of the cDNAs into mammalian expression vector, and prepared by a kind gift from other peoples and purchase (Origene). HT-29 cells were transfected with GFP and each cDNA for 24 h and hen exposed to TSI to induce necroptosis. Based on the morphology of GFP-positive necrotic cells, I first evaluated death rates of cells expressing kinases or phosphatases. Then, the secondary screening was assessed with similar assay but using with PI to determine the level of necroptosis.

2.2. Cell culture and stable cell lines

HT-29 cells were cultured in McCoy's 5A medium (Hyclone) and other cells were in Dulbecco’s Modified Eagles Medium (DMEM; Hyclone), supplemented with 10% defined FBS (Gibco) and 100 U/mL penicillin. Cells

were maintained in a 37 °C incubator at 5% CO2. HeLa cells were transfected with pcDNA3 encoding RIPK3-HA using iN-fect reagents (iNtRON Biotechnology) and selected with G418 (Sigma-Aldrich) to establish the HeLa/RIPK3-HA cell line. CK1γ knockout cells were generated using CRISPR/Cas9 system with LentiCRISPR (pXPR_001) that expresses each gene-targeting sgRNA. HeLa/RIPK-HA cells were transduced with the lentiviral delivery and selected with puromycin (Sigma-Aldrich).

2.3. Reagents and antibodies

The following chemicals were purchased: human TNFα (Merck Millipore); mouse TNFα (PeproTech); GSK'872, NSA, Nec1-s (Calbiochem); TRAIL (Invitrogen); Nec1, etoposide, tunicamycin, (Sigma-Aldrich). SM-164 was synthesized by Dr. Shaomeng Wang (University of Michigan). Gi was synthesized as described in Hua Z. et al., 2012. The antibodies used for the western blot analysis are: anti-RIPK3 (E1Z1D), anti-caspase-8, anti-His antibodies (Cell Signaling); anti-CK1γ2, anti-MLKL, anti-caspase-3, anti-

vimentin antibodies (Genetex); anti- PARP-1, anti-GST, anti-tubulin, anti-calnexin antibodies (Santa Cruz Biotechnology); anti-FLAG, anti-phospho-serine, anti-phospho-threonine antibodies (Sigma-Aldrich); anti-CK1γ1, anti-phospho-MLKL (p-S358) antibodies (Abcam); anti-RIPK1 antibody (BD Biosciences) and anti-CK1γ3 (Thermo Fisher Scientific). Anti-phospho-S344/345 CK1γ3 polyclonal antibody was generated against a peptide encoding the amino acid residues 339–350 of human CK1γ3. For the in vitro experiment, GST-RIPK3, GST-CK1γ1 (Sigma-Aldrich), GST-CK1γ3 (Abcam) and His-MLKL (Aviva Systems Biology) proteins were utilized.

2.4. Plasmid construction

RIPK3-HA was subcloned into pcDNA3-HA using following primers: 5'-HindIII, 5'-CCC AAG CTT ATG TCG TGC GTC AAG-3', 3'-KpnI, 5'-GGG GTA CCT TTC CCG CTA TGA TT-3' and FLAG-CK1γ1 into pCMV10 3x FLAG using primers: 5'-EcoRI, 5'-GGA ATT CCA AAC CTG ATT AT-3', 3'-KpnI, 5'-GGG GTA CCT CAC TTG TGG CGC TGA GCA GTC TTC TTC CTT TTC CTC

TTA AAG AAA CAG CAG CAC TTA GCT TCC TCC A-3' And FLAG-CK1γ3 was purchased from Sino Biological (Cat: HG10719-NF). CK1γ3 mutants (S344A, S345A, S344/345A and D162N) were generated by site-directed mutagenesis through PCR using primers containing the corresponding mutations: S344A-5', 5'-TCC TGC TCT GGC ATC AAA CAG-3'; S344A-3', 5'-CTG TTT GAT GCC AGA GCA GGA-3'; S345A-5', 5'-TCC TGC TCT GTC AGC AAA CAG AGA AGC-3'; S345A-3', 5'-TCC TGC TCT GTC AGC AAA CAG AGA AGC-3'; D162N-5', 5'-GAA CTT GAT ATA CAG AAA TGT AAA ACC TGA G-3'; D162N-3', 5'-CTC AGG TTT TAC ATT TCT GTA TAT CAA GTT C-3'. S344/354A mutant was made from S344A mutant with following primers. S344/354A-5', 5'- ATC CTG CTC TGG CAG CAA ACA GAG AAG-3', S344/354A-3', 5'- CTT CTC TGT TTG CTG CCA GAG CAG GAT-3'. All mutants were verified through DNA sequencing analysis.

2.5. shRNA-mediated knockdown.

First, shRIPK3 and shMLKL were subcloned into pSUPER neo using

following primers: shRIPK3-5', 5'- GAT CCC CCC ACT AGT CTG ACG GAT AAT TCA AGA GAT TAT CCG TCA GAC TAG TGG TTT TTA, shRIPK3-3', 5'- AGC TTA AAA ACC ACT AGT CTG ACG GAT AAT CTC TTG AAT TAT CCG TCA GAC TAG TGG GGG-3'; shMLKL-5', 5'- GAT CCC CCA AAC TTC CTG GTA ACT CAT TCA AGA GAT GAG TTA CCA GGA AGT TTG TTT TTA-3', shMLKL-3', 5'- AGC TTA AAA ACA AAC TTC CTG GTA ACT CAT CTC TTG AAT GAG TTA CCA GGA AGT TTG GGG-3'.

Each shRNA was transfected into HeLa/RIPK3-HA cells using iN-fect reagents. As a negative control, I used an empty pSUPER neo vector. After 72 h, HeLa/RIPK3-HA cells were stimulated with TSI and the level of proteins was confirmed by western blot or RT-PCR

2.6. Cell death assays

Cell viability was examined by staining nuclear chromatin with 1 μg/ml propidium iodide (PI; Sigma-Aldrich) or counting the number of GFP-positive cells before and after necroptosis induction under a fluorescence microscope

(Olympus). Apoptotic cell death was determined by trypan blue exclusion assays.

2.7. Immunoprecipitation and subcellular fractionation

Immunoprecipitation and subcellular fractionation were performed following the method previously described (Sun L, et al., 2012; Wang Z, et al., 2012) with minor modifications. Briefly, to gain S15 and P15 fractions, the harvested cells were resuspended with buffer A (20 mM Hepes pH 7.4, 40 mM KCl, 1.5 mM MgCl2, 1 mM EDTA, 1 mM EGTA, 0.1 mM PMSF and 250 mM sucrose) on ice and homogenized with a 22-G needle. After centrifugation at 1,000 x g for 10 min, the supernatant was again centrifuged at 15,000 x g for 10 min. The resulting supernatant was collected as S15 and the pellet was lyzed with lysis buffer (50 mM Tris pH 8.0, 137 mM NaCl, 1 mM EDTA, 1% Triton X-100, and 10% glycerol) and centrifugated to get the supernatant (P15). This P15 fraction was also used for immunoprecipitation assay with anti-CK1γ1 antibodies. The other half of the cells were lyzed with lysis buffer first, and the supernatant was saved as the whole cell

extract (WCL). The remaining pellet was resuspended with buffer S (20 mM Tris pH 7.4, 150 mM NaCl, and 1% SDS) and homogenized with a 22-G needle. After centrifugation, the supernatant was saved as SDS-sup.

2.8. *In vitro* binding assay

Recombinant proteins were incubated in cold phosphate buffered saline (PBS) with 1 mM DTT and 0.2 mM PMSF (Sigma-Aldridch) overnight at 4 °C and analyzed by immunoprecipitation (IP) assay using Ni-NTA beads (GE Healthcare), followed by western blotting.

2.9. *In vitro* kinase assay

Recombinant proteins were incubated in the kinase buffer (25 mM MOPS pH 7.2, 12.5 mM glycerol-2-phosphate, 25 mM MgC12, 5 mM EGTA, and 2 mM EDTA; 0.25 nM DTT was added just prior to use) for 2 h with 10 mCi [32p] ATP (PerkinElmer). The reaction mixtures were separated by SDS-PAGE and

transferred to nitrocellulose membrane after the loaded proteins were verified by Coomassie blue staining. Phosphorylations were identified by autoradiography analysis.

2.10. Statistical analysis

Results are expressed as mean ± S.E.M. ($n \geq 3$). All analyses were performed using SPSS Statistics ver.23 software.

3. RESULTS

3-1. CK1γ identified in a functional screen is involved in mediating TSI-induced necroptosis

To identify regulator(s) involved in the TNFα-induced necroptosis, I took an advantage of a cell-based functional assay with cDNA expression library. Because the phosphorylation is known to play an important role in regulating the activity of RIPK1 and RIPK3, I analyzed a collection of expression vectors for full-length cDNA encoding 650 kinases and 120 phosphatases using this gain-of-function (GOF) assay. HeLa cells stably expressing RIPK3-HA (HeLa/RIPK3-HA) were generated and transfected with an expression vector for each cDNA individually and then exposed to TNFα (T), Smac-mimetic (S) and IDN-6556 (I) to induce necroptosis. In this screening, CK1γ1 was identified as a promoter of necroptotic cell death. Because CK1γ has three isoforms (CK1γ1, CK1γ2 and CK1γ3), I tested effects of each CK1γ isoform on necroptosis. When ectopically overexpressed in HeLa/RIPK3-HA cells, both CK1γ1 and CK1γ3 significantly enhanced the cell

death, while CK1γ2 had no effect on this (Fig. 1A). To examine if CK1γ could also affect other types of cell death, I introduced apoptosis to Hela/RIPK3 cells with TNFα plus Smac-mimetic, etoposide or tunicamycin. In contrast to its effect on necroptosis, CK1γ1 had no effect on apoptosis induced under these conditions (Fig. 1B).

D4476 is a cell-permeable inhibitor widely used to block kinase activity of CK1 family (Rena G, et al., 2004), while Gi is a specific of inhibitor for CK1γ isoforms (Hua Z, et al., 2012). Using these CK inhibitors, I investigated the specific effect of CK1γ on necroptosis. Compared to necrostatin-1 (Nec1), an inhibitor of RIPK1 kinase activity (Degterev A, et al., 2005, 2008), Gi as well as D4476 exerted comparable and remarkable cytoprotection against TSI-induced necroptosis (Fig. 2A). In addition, I tested knockout the effects of CK1γs on the necroptosis. When CK1γ1 was knocked out alone using CRSPIR/Cas9 system in HeLa/RIPK3-HA cells, it had a partial rescue effect on the cell death (27% reduction). Interestingly, necroptotic cell death was more efficiently reduced by CK1γ3 knockdown in HeLa/RIPK3-HAcells (63% reduction). Compared to that

of CK1γ1 knockout or CK1γ3 knockdown alone, cell death was further suppressed by CK1γ1 and CK1γ3 double knockdown in HeLa/RIPK3-HA cells (84% reduction) (Fig 2B). These results suggest that both CK1γ1 and CK1γ3 are critical in TSI-induced necroptosis.

3-2. CK1γ1 is cleaved by caspase-8 *in vitro* and in apoptotic cells

RIPK1 and RIPK3 are known as targets of caspase-8 and are inactivated by cleavage during apoptosis. Similar to the cleavage of RIPK1 and RIPK3, I observed the cleavage of CK1γ1 during apoptosis. The cleavage product of CK1γ1 with molecular weight 37 kDa appeared in TNFα/Smac-mimetic (TS)-induced apoptotic HT-29 cells, but not in TSI-induced necrotic cells (Fig. 3A, *left*). PARP, a well-known caspase substrate, was also cleaved in the apoptotic cells. Likewise, the cleavage of CK1γ1 was also observed in HeLa cells undergoing TS-induced apoptosis but not in HeLa/RIPK3 cells undergoing necroptosis (Fig. 3A, *right*). These cleavages triggered by TS were no longer observed in the presence of pan-caspase inhibitor IDN (Fig. 3A and B). Deducing from size of the caspase

cleavage product and with the help of program to predict caspase cleavage motif, I chose Asp343 as a probable cleavage site. The results from mutagenesis analysis revealed that CK1γ1 D343A mutant replacing Asp343 with Ala was resistant to the cleavage during apoptosis (Fig. 3B). These results show that CK1γ1 is cleaved by caspase during apoptosis.

To identify caspase involved in the cleavage of CK1γ1, I examined effects of caspase inhibitors on the cleavage. Among them, z-IETD-fmk, an inhibitor of caspase-8, along with IDN, was most effective to prevent the cleavage of CK1γ1, while z-DEVD-fmk, an inhibitor of caspase-3, and z-AEVD-fmk, an inhibitor of caspase-10, showed less effectiveness (Fig. 4A). Next, I tested if candidate caspases could cleave CK1γ1 in a cell-free system. Recombinant RIPK3 protein was used a control target of caspase-8. Under this condition, both purified caspase-3 and caspase-8 cleaved CK1γ1 to produce GST-CK1γ1 cleavage product *in vitro* (Fig. 4B). On the other hand, the results from immunoprecipitation assay revealed that only caspase-8 interacted with CK1γ1 in apoptotic cells (Fig. 4C), indicating that CK1γ1 is cleaved by caspase-8 during apoptosis. In addition, I also checked

whether CK1γ3 was cleavable by caspase. Unlike CK1γ1, *in vitro* cleavage and apoptotic assays revealed that CK1γ3 was not cleaved by either caspase-3 or caspase-8 (Fig. 4B, data not shown). Collectively, CK1γ1 and CK1γ3 are regulated differently, at least, by caspase-8, although they act together in mediating necroptosis.

3-3. CK1γ1 and CK1γ3 are accumulated in response to TSI during necroptosis

In contrast to the cleavage of CK1γ1 during apoptosis, I found that CK1γ1 and CK1γ3 proteins accumulated in necroptotic cells. Compared to untreated control cells, the level of CK1γ1 or CK1γ3 increased 1.24- or 1.27-fold, respectively, in HeLa/RIPK3-HA cells when treated with TSI, while the amounts of CK1γ2 remained unchanged (Fig. 5). This result might be related to that from the experiment of overexpression of CK1γ1 CK1γ2 or CK1γ3 in Fig. 1A. In the same cells, I observed the activation of RIPK1 and RIPK3 and the phosphorylation of MLKL, confirming the activation of necroptotic complex

by TSI treatment. Interestingly, this accumulation of CK1γ1 and CK1γ3 proteins was suppressed by the treatment with a chemical inhibitor of RIPK1 (Nec1), RIPK3 (GSK'872), MLKL (NSA), CK1 (D4476) or CK1γ (Gi) (Fig. 6A). Similarly, I found that TSI-induced accumulation of CK1γ1 and CK1γ3 was abolished by knockdown of RIPK3 or MLKL expression in HeLa/RIPK3-HA cells (Fig. 6B). Moreover, unlike that in WT mouse embryo fibroblasts (MEFs), I observed lack of such accumulation of CK1γ1 and CK1γ3 in RIPK1 and MLKL knockout MEFs (Fig. 6C). Therefore, it is thought that the increase of CK1γ1 and CK1γ3 proteins by TSI may be associated with necroptosis progression.

To address how CK1γ1 and CK1γ3 might be accumulated in cells in response to TSI, I investigated if the stability of CK1γ1 and CK1γ3 proteins might be increased by binding to each other or forming a protein complex in necroptotic cells, as seen in the formation of MLKL trimer or tetramer which is important to induce necroptosis. I found that under non-reducing SDS-PAGE, FLAG-CK1γ1 and FLAG-CK1γ3 could form oligomers in the cells treated with

TSI (Fig. 7A). While these oilgomers of CK1γ were detectable before TSI treatment, their amounts increased during necroptosis. Under this necroptotic condition, MLKL also formed oligomers. Moreover, I observed the homolytic and heterolytic interactions between CK1γ1 and CK1γ3, when they were ectopically expressed in HEK 293T cells (Fig. 7B and C).

3-4. CK1γ is a component of necrosome harboring active RIPK1, RIPK3 and MLKL

Next, I examined if CK1γ was a component of the necrosome complex. To test this possibility, immunoprecipition assay was performed using anti-CK1γ1 antibody first because CK1γ3 was not detected in the 1% triton X-100-soluble fraction (WCL in Fig. 9). The results revealed that upon treatment with TSI, CK1γ1 was recruited into the immunocomplex containing RIPK1, RIPK3 and MLKL in HeLa/RIPK3-HA cells (Fig. 8A). Similarly, I found the protein complex harboring active CK1γ1, RIPK3 and MLKL in HT-29 cells undergoing TSI-induced necroptosis (Fig. 8B). To verify the interaction among them, *in vitro*

binding assay using purified proteins was followed. When His-MLKL was pulled-down using Ni-NTA beads, only little amounts of CK1γ1 were detected in the MLKL complex no matter what RIPK3 was incubated together or not. One interesting thing to note was that the binding of RIPK3 to MLKL was enhanced by the presence of CK1γ1 (Fig. 8C). However, compared to that of MLKL and RIPK3, the interaction between MLKL and CK1γ1 was relatively weak. CK1γ3 also showed similar patterns with CK1γ1 (data not shown). Together, these results imply that CK1γ1 or CK1γ3 might bind to RIPK3, rather than MLKL, enhancing the formation of MLKL and RIPK3 complex.

It is known that activated RIPK1 and RIPK3 by necroptotic stimuli form amyloid-like structure which is found in highly insoluble fraction (Li J, et al., 2012; Wang H, et al., 2014). With cellular fractionation assay, I thus examined whether CK1γ could bind to necrosome in the insoluble fraction. As previously reported, RIPK1, RIPK3 and MLKL moved to more insoluble fraction (P15 or SDS-sup), when stimulated by necroptotic stimuli (Fig. 9). On the other hand, subcellular localizations of CK1γs were not changed upon necroptosis. CK1γ1

was located mainly in the 1% triton X-100-soluble fraction (WCL) and some in the P15 and the SDS-sup fractions, and CK1γ3 was detected only in the SDS-supernatant fractions (SDS-sup) where active necrosomes were localized most abundantly. Unlike CK1γ1 and CK1γ3, CK1γ2 was exclusively found in the S15, a faction whose components were most soluble. Thus, these results suggest that CK1γ1 and CK1γ3 might function in necroptosis after activated RIPK1, RIPK3 and MLKL move to where CK1γ is located.

3-5. CK1γ is autophosphorylated and phosphorylates RIPK3 to activate it *in vitro*

Because both RIPK3 and CK1γ are protein kinases, I examined if one kinase phosphorylated the other *in vitro*. In advance, I found that CK1γ1 or CK1γ3, as well as RIPK3, was autophosphorylated by itself (Fig. 10A, *upper*). More importantly, I observed that compared to RIPK3 alone (lane 1), the phosphorylation of RIPK3 was enhanced by 1.5- and 1.7- fold when it was incubated together with CK1γ1 (lane 4) or CK1γ3 (lane 5), respectively (Fig. 10A,

lower). It seemed that the phosphorylation of CK1γ1 and CK1γ3 also was somewhat enhanced when they were incubated with RIPK3. I then decided to identify the kinases responsible for these phosphorylations using the chemical inhibitors against RIPK3 (GSK'872) or CK1γ (Gi) (Fig. 10B). I confirmed that Gi did not affect the phosphorylation of RIPK3 and GSK'872 did not inhibit CK1γ (Fig. 10B, *lower*). When the reaction mixtures of RIPK3 and CK1γ1 or RIPK3 and CK1γ3 were incubated with GSK'872 or Gi, only Gi reduced the phosphorylation of RIPK3 *in vitro* (lane 6 and 9), while GSK'872 did not affect the phosphorylation of those kinases (lane 5 and 8). Therefore, I conclude that CK1γ phosphorylates RIPK3.

It is still not certain whether the enhanced phosphorylation of RIPK3 by CK1γ results in the activation of RIPK3 or not. Once RIPK3 is activated in necroptotic cells, it phosphorylates MLKL and the phosphorylated MLKL subsequently forms oligomers and makes pores in the plasma membrane (Wang H, et al., 2014). Unfortunately, in the same kinase assay I could not detect the phosphorylation of MLKL which was incubated with RIPK3. As an alternative choice, the analysis

using non-reducing SDS-PAGE revealed that the treatment with Gi appeared to impede the oligomerization of MLKL in necroptotic cells (Fig. 11). As reported, Nec1 also blocked the formation of MLKL oligomers of MLKL in the same assay. Together, these results imply that CK1γ stimulates the activation of MLKL probably through RIPK3 during necroptosis.

3-6. CK1γ3 is autophosphorylated at Ser344 and 345 to exert its activity in necroptosis

When CK1γ3 were overexpressed in cells, I found slow-migrating CK1γ3 on SDS-protein gel (Fig. 12A). The levels of slow-migrating CK1γ3 were not visually changed upon stimulation with TSI. Given CK1γ1 and CK1γ3 were autophosphorylated in an *in vitro* assay (Fig. 10A) and a kinase dead mutant of CK1γ3 (D162N) did not show these retardations of migration in SDS-PAGE (Fig. 12A), the slow-migrating CK1γ3 was considered as phosphorylated forms of CK1γ3 at Ser and Thr residues (Fig. 12B). To find out the residues of CK1γ3 for

autophosphorylation, I generated many CK1γ3 mutants replacing Ser/Thr with Ala. Among them, I found that introduction of the mutations at Ser344 and 345 (CK1γ3-S344/345A) reduced the shift on the protein gel compared to CK1γ3 WT (Fig. 12A), although autophosphorylation was not totally blocked, like in CK1γ3 D162N mutant (Fig. 12B). I confirmed this phosphorylation at Ser344/345 with the help of liquid chromatography tandem-mass spectrometry (LC-MS/MS) experiments. Phosphorylated peptides of CK1γ3 at Ser344 and Ser345 were increased in HeLa/RIPK3-HA cells treated with TSI compared to untreated control (25 or 42 %, respectively, Table 1).

I also investigated a role of this phosphorylated CK1γ3 in necroptosis and found that compared to CK1γ3 WT, CK1γ3-S344/345A mutant significantly lost the ability to enhance TSI-induced necroptosis (Fig. 12C). I then decided to generate an antibody detecting the phosphorylated form of CK1γ3 at Ser344/345 (CK1γ3 p2S). From western blot analysis, the antibody against CK1γ3 p2S well recognized CK1γ3 WT, but not CK1γ3-S344A, CK1γ3-S345A and CK1γ3-

S344/345A mutants as well as CK1γ3-D162N mutant (Fig. 13). However, it was hard to find any significant differences in total levels of phosphorylated CK1γ3 (CK1γ3 p2S) between untreated and TSI-treated cells. There was only a marginal increase of CK1γ3 p2S that just corresponded to the elevated levels of total CK1γ3 in necroptotic cells (Fig. 14). Thus, I chose an alternative way employing an immunoprecipitation assay of necrosome and found that the phosphorylated CK1γ3 at Ser344/345 clearly was clearly detected only in RIPK3-containing necrosome of necroptotic cells (Fig. 15). It thus appears that antophosphorylated form of CK1γ3 at Ser344/345 is found in necrosome to mediate necroptosis.

3-7. Gi protects mice in a TNFα-induced systemic inflammatory response syndrome (SIRS) model

The absence of RIPK1 kinase activity or genetic deletion of RIPK3 has been proven to be protective against TNFα-induced hypothermia and survival of mice (Duprez L, et al., 2011; Newton K, et al., 2014). I next examined *in vivo*

contribution of CK1γ-mediated necroptosis to a TNFα-induced systemic inflammatory response syndrome (SIRS) model. As reported, the injection of mice with mouse form of TNFα (mTNFα) alone through the tail vein caused abrupt death of the mice with hypothermia (Fig. 16A and B). On the other hand, prior injection with 7-Cl-O-Nec-1, referred to as Nec1-s, a more stable analogue of Nec1 (Degterev A, et al., 2008, 2013), protected the mice from the death and the hypothermia. When I injected mice with CK1γ inhibitor Gi prior to challenge with mTNFα, I found that Gi pretreatment also improved the survival rate of mice in TNFα-treated group (Fig. 16A) and ameliorated the hypothermia, though its effects were a little less than Nec1-s (Fig. 16B). These results suggest that CK1γ inhibitor Gi protects mice in SIRS model but is less potent than Nec1-s, as consistent with the results from cell-based assays.

Figure 1. Functional isolation of CK1γ as a regulator promoting TSI-induced necroptosis. (**A**) Ectopic expression of CK1γ1 or CK1γ3 enhances necroptosis. HeLa cells stably expressing RIPK3-HA was co-transfected with EGFP and either pcDNA3 (control), CK1γ1, CK1γ2 or CK1γ3 for 24 h, and then treated with 10 ng/mL TNFα (T), 100 nM Smac-mimetic (S) and 10 μM IDN-6556 (I) for 4 h. Cell death rates were determined by counting the number of GFP-positive cells. n.s.; not significant. (**B**) Overexpression of CK1γ1 does not affect apoptosis. HeLa cells were left untreated (NT) or treated with 20 ng/mL TNFα + 100 nM SM-164 for 6 h, 100 μM etoposide for 24 h or 8 μg/ml tunicamycin for 48 h. Cell viability was determined by trypan blue exclusion assay (*left*) and the expression of HA-Bcl-2 or FLAG-CK1γ1 was confirmed by western blotting (*right*).

Figure 1.

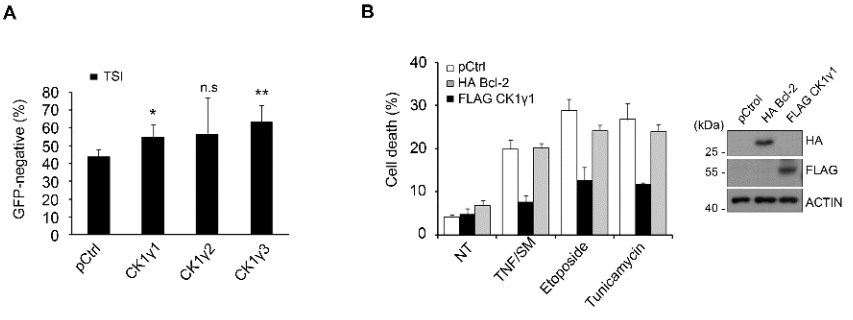
A
TSI
GFP-negative (%)
80
70
60
50
40
30
20
10
0
*
n.s
**
pCtrl
CK1γ1
CK1γ2
CK1γ3
B
pCtrl
HA Bcl-2
FLAG CK1γ1
Cell death (%)
40
30
20
10
0
NT
TNF/SM
Etoposide
Tunicamycin
(kDa)
pCtrl
HA Bcl-2
FLAG CK1γ1
25
55
40
HA
FLAG
ACTIN

Figure 2. Downregulation of CK1γ attenuates necroptosis. (**A**) CK1γ inhibitor blocks necroptosis. HeLa/RIPK3-HA cells were treated for 3.5 h with TSI in the presence or absence of 10 μM Nec1, GSK'872, NSA, D4476 or Gi. Cell death rates were determined by counting propidium iodide (PI)-positive cells. (**B**) Knockdown of CK1γ1 and 3 expression inhibits necroptosis. HeLa/RIPK3-HA/CK1γ knockout (sgCK1γ1, 3 or both 1 and 3) cells were treated with TSI for 3.5 h (*left*). The expression levels of CK1γ1 and CK1γ3 were detected by immunoblotting (*below)*. Bars represent the mean ± SEM from at least three independent experiments. *$p< 0.05$, **$p< 0.01$, ***$p< 0.0001$.

Figure 2.

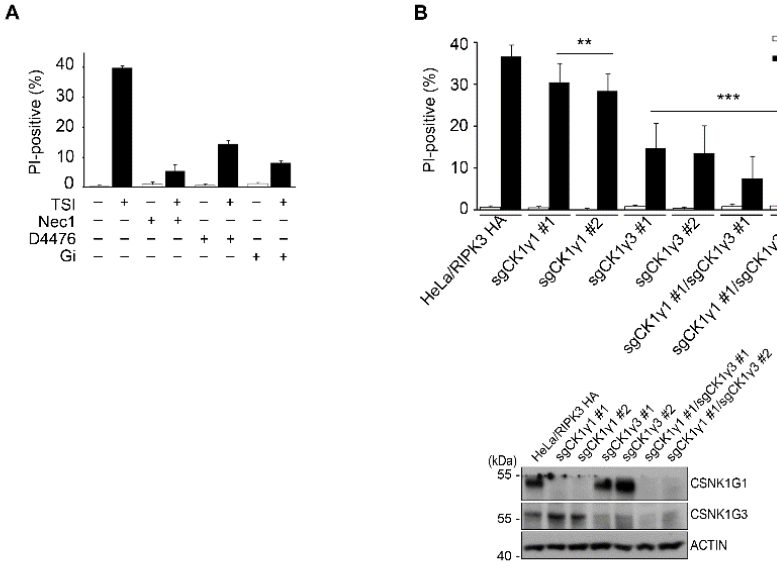
A
PI-positive (%)
40
30
20
10
0
TSI
Nec1
D4476
Gi
B
PI-positive (%)
NT
TSI
**
***
HeLa/RIPK3 HA
sgCK1γ1 #1
sgCK1γ1 #2
sgCK1γ3 #1
sgCK1γ3 #2
sgCK1γ1 #1/sgCK1γ3 #1
sgCK1γ1 #1/sgCK1γ3 #2
(kDa)
55
55
40
CSNK1G1
CSNK1G3
ACTIN

Figure 3. CK1γ1 is cleaved in apoptotic cells. (**A**) CK1γ1 is cleaved during apoptosis. HT-29 (left), HeLa and HeLa/RIPK3-HA (*right*) cells were treated for 5 h with 20 ng/mL TNFα and 100 nM Smac-mimetic (TS) to induce apoptosis (*left*) or for 3 h 10 ng/mL TNFα, 100 nM Smac-mimetic and 10 μM IDN-6556 (TSI) to induce necroptosis. Cell extracts were analyzed by western blotting. (**B**) CK1γ1 is cleaved at Asp343 by caspase. HeLa cells were transfected with FLAG-CK1γ1 WT or non-cleavable CK1γ1 D343A mutant for 24 h, exposed to TS in the presence or absence of 10 μM IDN for 6h and cell extracts were examined by western blotting.

Figure 3.

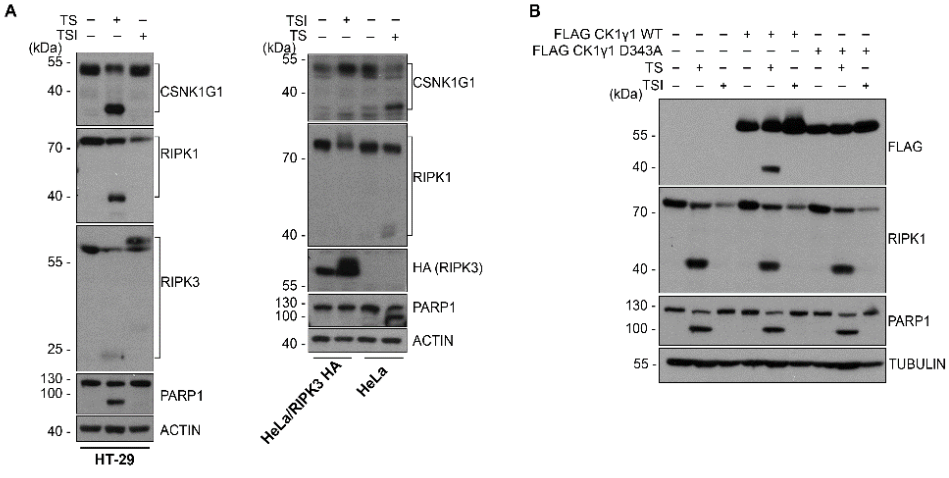
A
TS
TSI
(kDa)
55
40
70
40
55
25
130
100
40
CSNK1G1
RIPK1
RIPK3
PARP1
ACTIN
HT-29
HeLa/RIPK3 HA
HeLa
HA (RIPK3)
B
FLAG CK1γ1 WT
FLAG CK1γ1 D343A
FLAG
TUBULIN

Figure 4. CK1γ1 is cleaved by caspase-8 *in vitro*. (**A**) CK1γ1 cleavage is inhibited by caspase-8 or 3 inhibitor. HeLa cells were treated with TS in the presence of the indicated caspase inhibitor (10 μM). (**B**) CK1γ1 is cleaved by caspase-8 or caspase-3 *in vitro*. Recombinant GST-RIPK3, GST-CK1γ1 and GST-CK1γ3 proteins were incubated for 2 h with purified caspase-3 or caspase-8 protein for *in vitro* cleavage assay. (**C**) CK1γ1 binds to active caspase-8, not to caspase-3 or caspase-10, in apoptotic cells. HeLa/RIPK3-HA cells were treated with 20 ng/mL TNFα + 100 nM SM-164 for 6 h and analyzed by immunoprecipitation (IP) assay using anti-CK1γ1 antibody.

Figure 4.

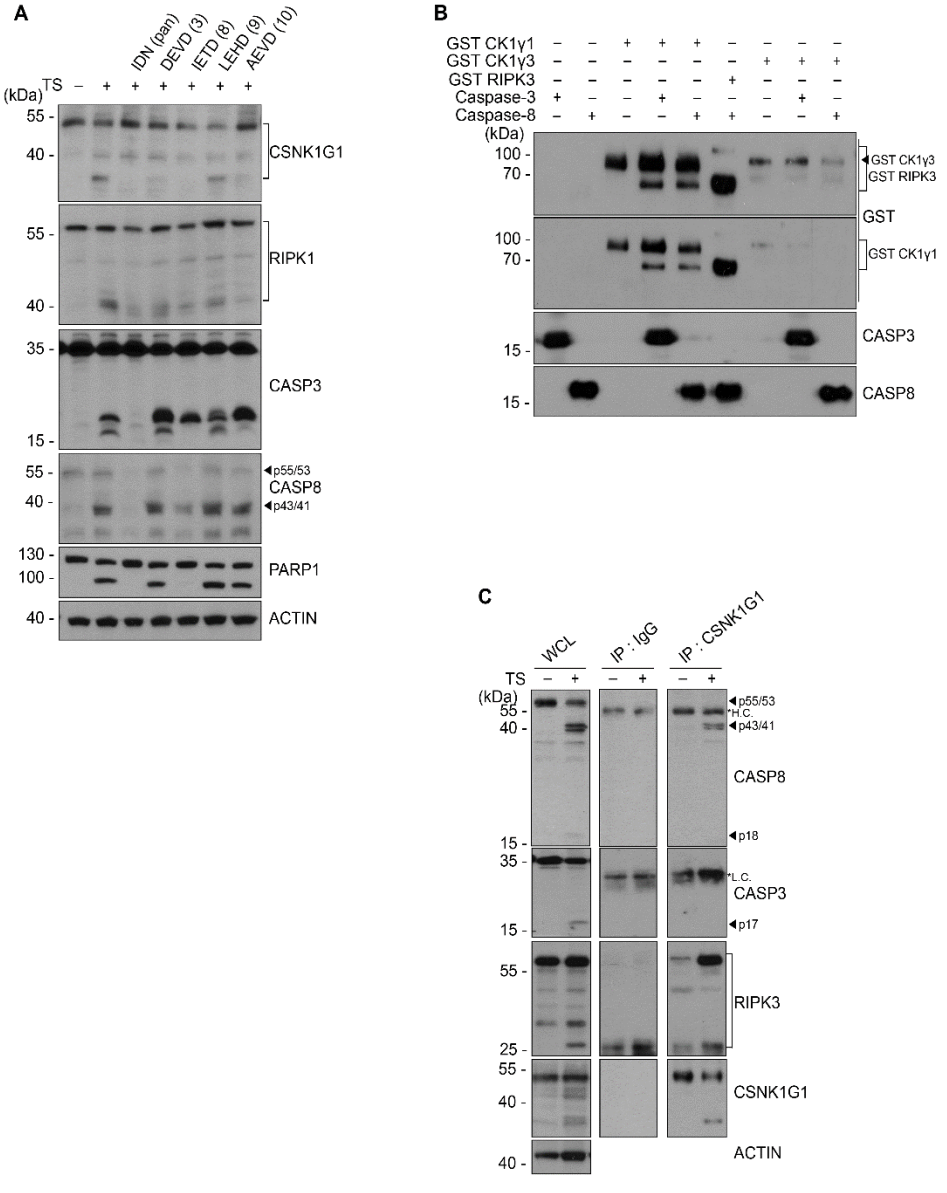
A
IDN (pan)
DEVD (3)
IETD (8)
LEHD (9)
AEVD (10)
TS
(kDa)
55 -
40 -
CSNK1G1
55 -
40 -
RIPK1
35 -
15 -
CASP3
55 -
40 -
p55/53
CASP8
p43/41
130 -
100 -
PARP1
40 -
ACTIN
B
GST CK1γ1
GST CK1γ3
GST RIPK3
Caspase-3
Caspase-8
(kDa)
100 -
70 -
GST CK1γ3
GST RIPK3
GST
100 -
70 -
GST CK1γ1
15 -
CASP3
15 -
CASP8
C
WCL
IP : IgG
IP : CSNK1G1
TS
(kDa)
55 -
40 -
p55/53
*H.C.
p43/41
CASP8
p18
15 -
35 -
*L.C.
CASP3
p17
15 -
55 -
RIPK3
25 -
55 -
40 -
CSNK1G1
40 -
ACTIN

Figure 5. The amounts of CK1γ1 or CK1γ3, but not CK1γ2, are elevated in necrotic cells. HeLa/RIPK3-HA cells were treated with TSI for 4 h. The expression levels of CK1γ1, CK1γ2 and CK1γ3 were detected by immunoblotting (*left*). Bars represent the mean ± SEM from at least three independent experiments (*right*). *$p < 0.05$.

Figure 5.

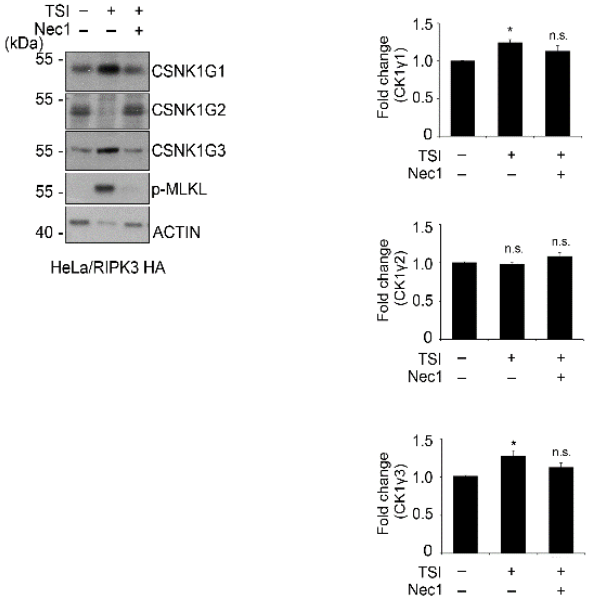
TSI – + +
Nec1 – – +
(kDa)
55 -
CSNK1G1
55 -
CSNK1G2
55 -
CSNK1G3
55 -
p-MLKL
40 -
ACTIN
HeLa/RIPK3 HA
Fold change (CK1γ1)
Fold change (CK1γ2)
Fold change (CK1γ3)
1.5
1.0
0.5
0
*
n.s.
TSI – + +
Nec1 – – +

Figure 6. The accumulation of CK1γ during necroptosis is inhibited by downregulation of RIPK1, RIPK3 or MLKL. (**A**) A chemical inhibitor of RIPK1, RIPK3 or MLKL blocks the accumulation of CK1γ1 and CK1γ3 in necroptotic cells. HeLa/RIPK3-HA cells were treated with 10 ng/mL TNFα, 100 nM Smac-mimetic and 10 μM IDN-6556 (TSI) in the presence or absence of 10 μM Nec1, GSK'872, NSA, D4476 or Gi for 3.5 h and analyzed by western blotting. (**B, C**) CK1γ1 and CK1γ3 accumulation triggered by TSI is impaired by Nec1 or downregulation of RIPK1, RIPK3 or MLKL. HeLa/RIPK3-HA cells were transfected with control shRNA (-) or shRNA targeting RIPK3 or MLKL for 48 h and treated with TSI in the presence or absence of 10 μM Nec1 for 3.5 h (B). RIPK1 or MLKL knockout (-/-) MEFs were treated with 20 ng/mL mouse TNFα (mTNFα), 100 nM Smac-mimetic and 10 μM IDN-6556 for 4 h (C). Cell extracts were analyzed by western blotting.

Figure 6.

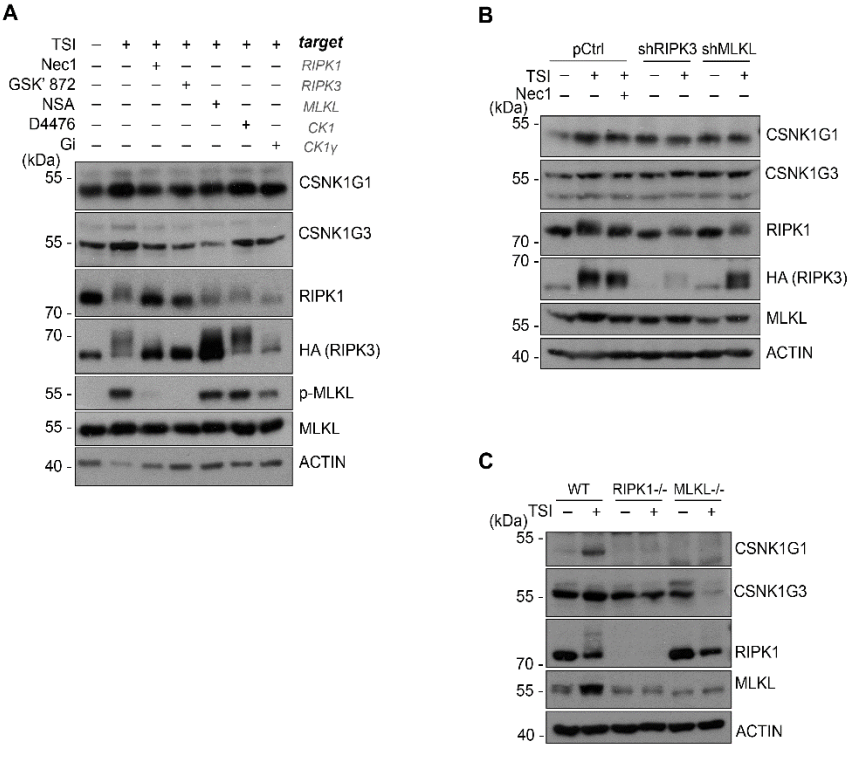
A
TSI
Nec1
GSK' 872
NSA
D4476
Gi
target
RIPK1
RIPK3
MLKL
CK1
CK1γ
(kDa)
55
CSNK1G1
55
CSNK1G3
70
RIPK1
70
HA (RIPK3)
55
p-MLKL
55
MLKL
40
ACTIN
B
pCtrl
shRIPK3
shMLKL
TSI
Nec1
(kDa)
55
CSNK1G1
55
CSNK1G3
70
RIPK1
70
HA (RIPK3)
55
MLKL
40
ACTIN
C
WT
RIPK1-/-
MLKL-/-
TSI
(kDa)
55
CSNK1G1
55
CSNK1G3
70
RIPK1
55
MLKL
40
ACTIN

Figure 7. CK1γ1 and CK1γ3 form either homo- or hetero-dimer. (**A**) CK1γ1 or CK1γ3 forms dimer. HeLa/RIPK3-HA cells were transfected with FLAG-CK1γ1 or CK1γ3, and then treated with TSI for 3 h. Cell extracts were separated by SDS-PAGE under non-reducing condition and analyzed by western blotting. (**B, C**) GFP-CK1γ1 makes up homocomplex with FLAG-CK1γ1 and heterocomplex with FLAG-CK1γ3.HEK 293T cells were cotransfected withGFP-CK1γ1 and FLAG-CK1γ1 (B) or GFP-CK1γ1 and FLAG-CK1γ3 (C), and subjected to immunoprecipitation (IP) assay with anti-FLAG beads. Whole cell lysates (WCL) and the immunoprecipitants were analyzed by western blotting.

Figure 7.

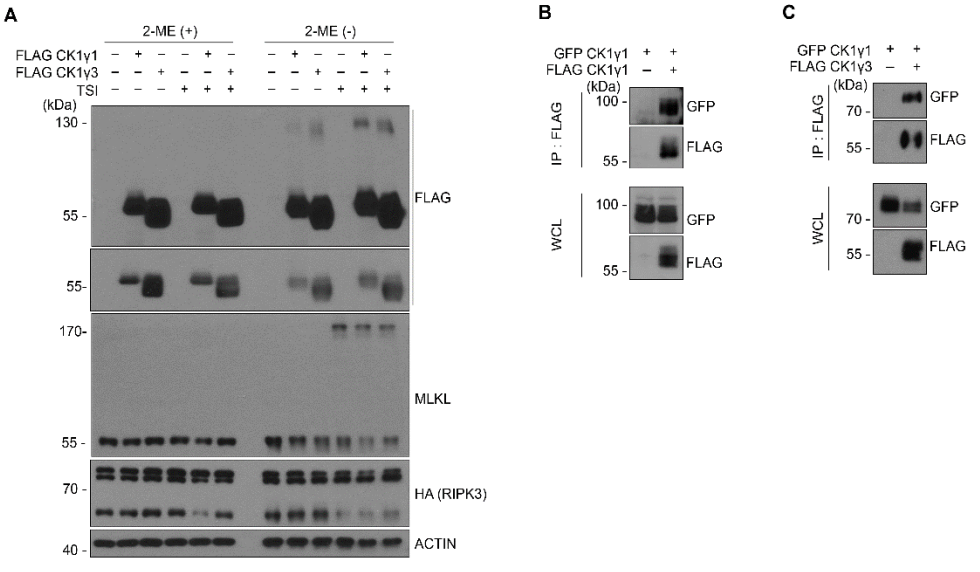
A
2-ME (+)
2-ME (-)
FLAG CK1γ1
FLAG CK1γ3
TSI
(kDa)
130 -
55 -
55-
170-
55 -
70 -
40 -
FLAG
MLKL
HA (RIPK3)
ACTIN
B
GFP CK1γ1
FLAG CK1γ1
(kDa)
IP : FLAG
WCL
100 -
55 -
GFP
FLAG
C
GFP CK1γ1
FLAG CK1γ3
(kDa)
IP : FLAG
WCL
70 -
55 -
GFP
FLAG

Figure 8. CK1γ interacts with necrosome. (**A, B**) CK1γ1 interacts with RIPK1, RIPK3 and MLKL in necrotoptic cells. HeLa/RIPK3-HA or HeLa/RIPK3-HA/CK1γ1 knockdown (A) or HT-29 (B) cells were treated with TSI for 3 h (A) or 6 h (B), respectively and analyzed by immunoprecipitation (IP) assay with anti-CK1γ1 antibody. The immunoprecipitates (*upper*) and whole cell lysates (WCL) (*lower*) were analyzed by western blotting. (**C**) *In vitro* binding assay showing binding of CK1γ to MLKL and RIPK3. Recombinant His-MLKL, GST-RIPK3 and GST-CK1γ1proteins were incubated overnight at 4 ℃ as indicated and analyzed by immunoprecipitation (IP) assay using Ni-NTA beads.

Figure 8.

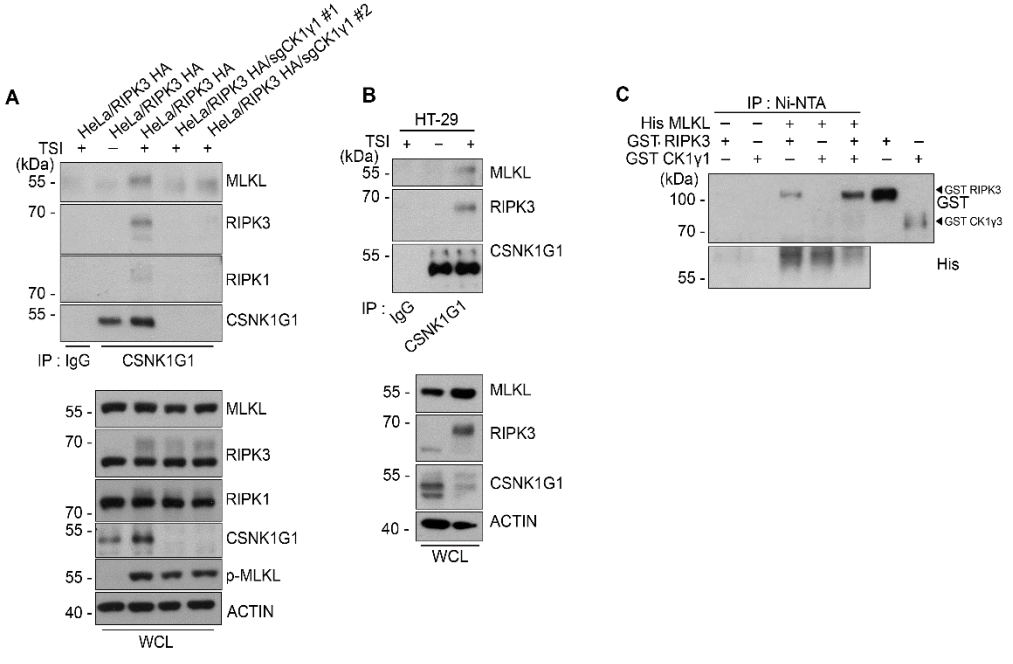
A
HeLa/RIPK3 HA
HeLa/RIPK3 HA
HeLa/RIPK3 HA
HeLa/RIPK3 HA/sgCK1γ1 #1
HeLa/RIPK3 HA/sgCK1γ1 #2
TSI + − + + +
(kDa)
55 -
MLKL
70 -
RIPK3
RIPK1
70 -
55 -
CSNK1G1
IP : IgG
CSNK1G1
55 -
MLKL
70 -
RIPK3
RIPK1
70 -
55 -
CSNK1G1
55 -
p-MLKL
40 -
ACTIN
WCL
B
HT-29
TSI + − +
(kDa)
55 -
MLKL
70 -
RIPK3
55 -
CSNK1G1
IP :
IgG
CSNK1G1
55 -
MLKL
70 -
RIPK3
55 -
CSNK1G1
40 -
ACTIN
WCL
C
IP : Ni-NTA
His MLKL − − + + +
GST-RIPK3 + − + − + + −
GST CK1γ1 − + − + + − +
(kDa)
100 -
GST RIPK3
GST
GST CK1γ3
70 -
55 -
His

Figure 9. CK1γ1 and CK1γ3 are found in a subcellular fraction harboring active RIPK1, RIPK3 and MLKL. CK1γ1 and CK1γ3 are detected in a highly insoluble fraction harboring RIPK1, RIPK3 and MLKL. HeLa/RIPK3-HA cells were treated with TSI for 3 h and fractionated by centrifugations at 15,000 rpm into supernatant (S15) and pellet (P15) or WCL and SDS-sup fractions, which were obtained from the pellets of WCL and dissolved by 1% SDS first, then further diluted with lysis buffer to 0.1% SDS. Each cellular fraction was analyzed by western blotting.

Figure 9.

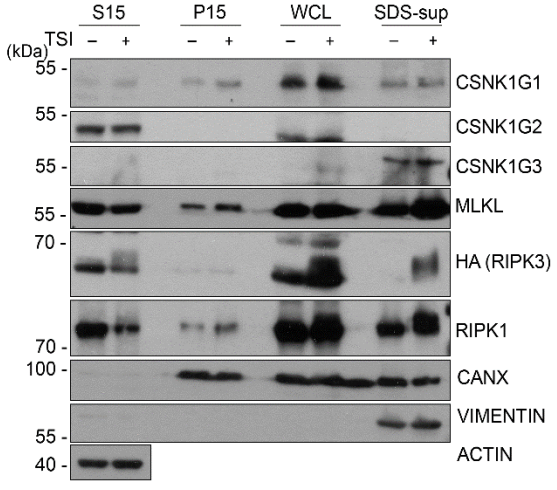
S15
P15
WCL
SDS-sup
TSI
– + – + – + – +
(kDa)
55 -
55 -
55 -
55 -
70 -
70 -
100 -
55 -
40 -
CSNK1G1
CSNK1G2
CSNK1G3
MLKL
HA (RIPK3)
RIPK1
CANX
VIMENTIN
ACTIN

Figure 10. CK1γ is auto-phosphorylated and phosphorylates RIPK3 *in vitro*.

(**A**) *In vitro* kinase assay showing CK1γ autophosphorylation and enhanced phosphorylation of RIPK3 by CK1γ. Recombinant GST-RIPK3, GST-CK1γ1 and GST-CK1γ3 proteins were incubated as indicated for 2 h in a kinase assay with 10 mCi [^{32}p] ATP. The reaction mixtures were separated by SDS-PAGE and transferred to nitrocellulose membrane, followed by autoradiography (*upper*). Purified proteins used were stained by Coomassie blue (*middle*). Bars represent the mean ± SEM from at least three independent experiments (*lower*). *p< 0.01, **p< 0.001. (**B**) CK1γ inhibitor Gi blocks RIPK3 phosphorylation by CK1γ (*upper*), but not RIPK3 auto-phospharylation (*lower left*). The same kinase assays were performed in the absence or presence of 20 μM GSK'872 or Gi.

Figure 10.

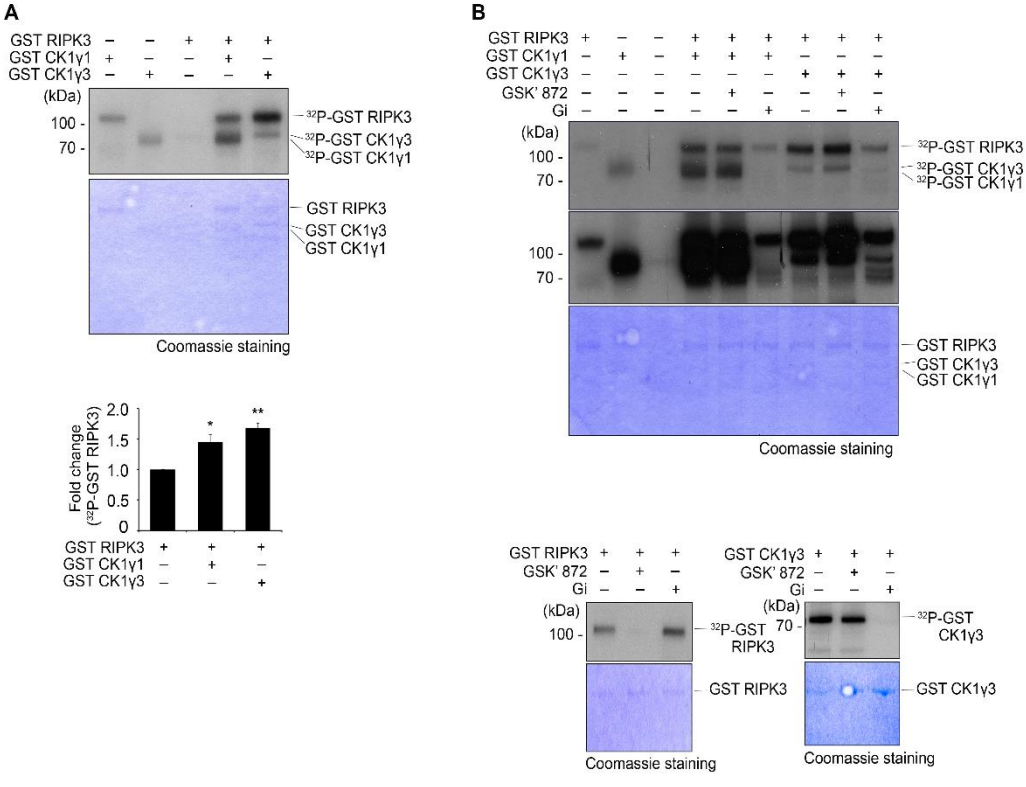
A
GST RIPK3 – – + + +
GST CK1γ1 + – – + –
GST CK1γ3 – + – – +
(kDa)
100 -
70 -
32P-GST RIPK3
32P-GST CK1γ3
32P-GST CK1γ1
GST RIPK3
GST CK1γ3
GST CK1γ1
Coomassie staining
Fold change (32P-GST RIPK3)
2.0
1.5
1.0
0.5
0
*
**
GST RIPK3 + + +
GST CK1γ1 – + –
GST CK1γ3 – – +
B
GST RIPK3 + – – + + + + + +
GST CK1γ1 – + – + + + – – –
GST CK1γ3 – – – – – – + + +
GSK' 872 – – – – + – – + –
Gi – – – – – + – – +
(kDa)
100 -
70 -
32P-GST RIPK3
32P-GST CK1γ3
32P-GST CK1γ1
100 -
70 -
GST RIPK3
GST CK1γ3
GST CK1γ1
Coomassie staining
GST RIPK3 + + +
GSK' 872 – + –
Gi – – +
(kDa)
100 -
32P-GST RIPK3
GST RIPK3
Coomassie staining
GST CK1γ3 + + +
GSK' 872 – + –
Gi – – +
(kDa)
70 -
32P-GST CK1γ3
GST CK1γ3
Coomassie staining

Figure 11. CK1γ inhibitor Gi blocks MLKL oligomerization. HeLa/RIPK3-HA cells were treated with TSI for 3 h in the presence or absence of 10 μM Nec1 or Gi for 3 h. Cell extracts were separated by SDS-PAGE under non-reducing condition and analyzed by western blotting.

Figure 11

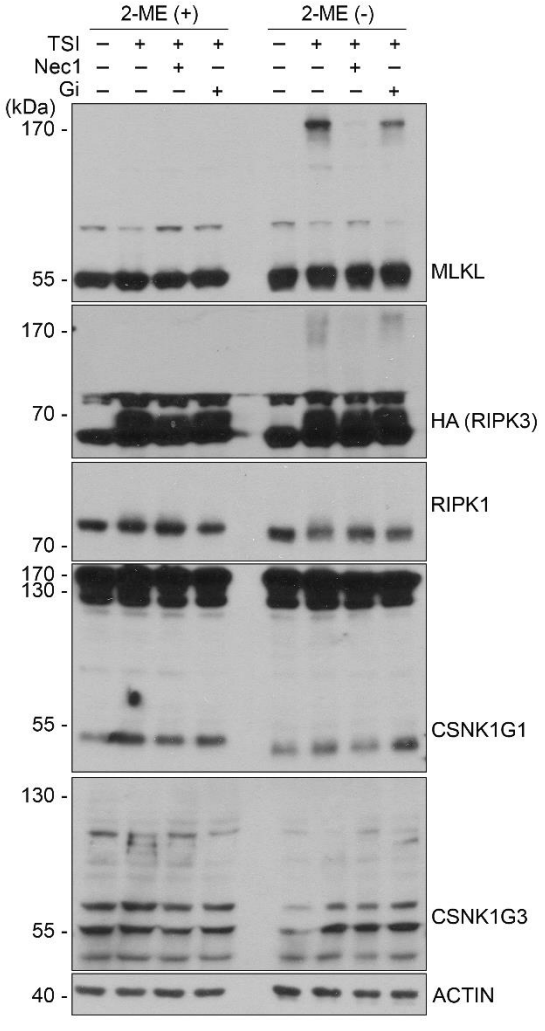
2-ME (+)
2-ME (-)
TSI
Nec1
Gi
(kDa)
170 -
55 -
MLKL
170 -
70 -
HA (RIPK3)
RIPK1
70 -
170 -
130 -
55 -
CSNK1G1
130 -
55 -
CSNK1G3
40 -
ACTIN

Figure 12. CK1γ3 autophosphorylation occurs at Ser344 and 345 and is important for necroptosis. (**A**) Overexpressed CK1γ3 undergoes autophosphorylation at Ser344 and 345. HeLa/RIPK3-HA cells were transfected with FLAF-CK1γ3 WT or mutants for 24h and treated with TSI for 3 h. (**B**) Mutations at Ser344 and 345 impedes CK1γ3 autophosphorylaiton. HEK 293T cells were transfected with either FLAG-CK1γ3 WT or its mutants. Cells lysates were analyzed by immunoprecipitation (IP) assay with anti-FLAG beads followed by western blotting using phospho-Ser or Thr antibody. The immunoprecipitants (*upper*) and whole cell lysates (*lower*) were analyzed by western blotting. (**C**) Overexpression of CK1γ3 Ser344/345Ala mutant reduces necroptosis. HeLa/RIPK3-HA cells were cotransfected with EGFP and either CK1γ3 WT or mutants for 24 h, and treated with TSI for 4 h. Cell death rates were determined by counting the number of GFP-positive cells. Bars represent the mean ± SEM from at least three independent experiments. $*p < 0.05$.

Figure 12.

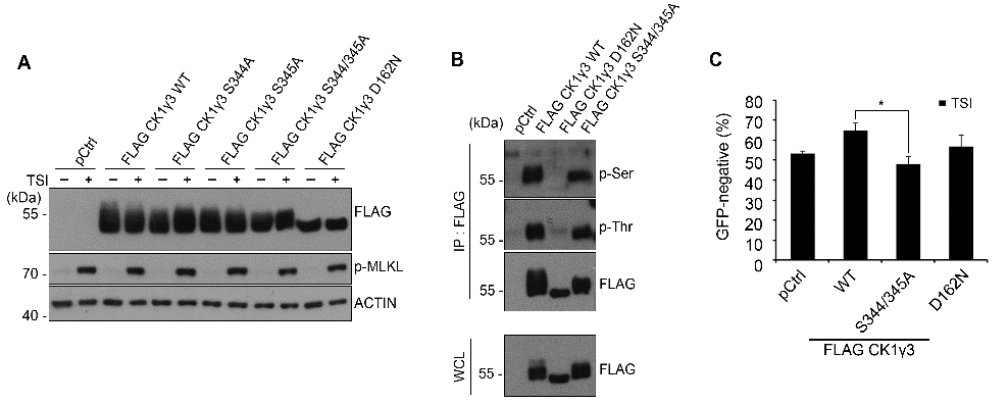
A
pCtrl
FLAG CK1γ3 WT
FLAG CK1γ3 S344A
FLAG CK1γ3 S345A
FLAG CK1γ3 S344/345A
FLAG CK1γ3 D162N
TSI
(kDa)
55
70
40
FLAG
p-MLKL
ACTIN
B
(kDa)
pCtrl
FLAG CK1γ3 WT
FLAG CK1γ3 D162N
FLAG CK1γ3 S344/345A
IP : FLAG
55
p-Ser
55
p-Thr
55
FLAG
WCL
55
FLAG
C
GFP-negative (%)
80
70
60
50
40
30
20
10
0
*
TSI
pCtrl
WT
S344/345A
D162N
FLAG CK1γ3

Figure 13. Generation of CK1γ3 p-2S antibody recognizing the phosphorylation at Ser344/345 of CK1γ3. HEK 293T cells were transfected with either FLAG-CK1γ3 WT or mutants and analyzed by immunoprecipitation (IP) assay with anti-FLAG beads, followed by western blotting using CK1γ3 p-2S antibody.

Figure 13.

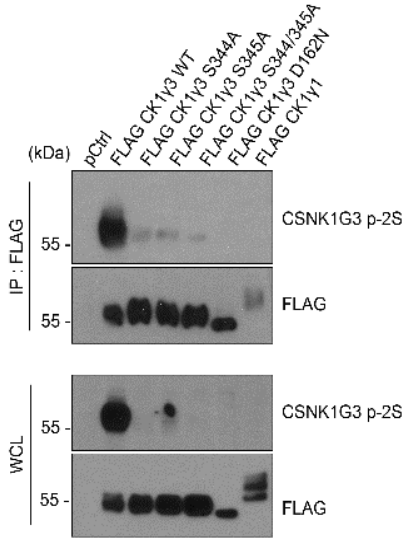
(kDa)
pCtrl
FLAG CK1γ3 WT
FLAG CK1γ3 S344A
FLAG CK1γ3 S345A
FLAG CK1γ3 S344/345A
FLAG CK1γ3 D162N
FLAG CK1γ1
IP : FLAG
55
55
CSNK1G3 p-2S
FLAG
WCL
55
55
CSNK1G3 p-2S
FLAG

Figure 14. Phosphorylated form of CK1γ3 at S344/345 is not significantly increased in necroptotic cells. HeLa/RIPK3-HA (A) or HT-29 cells (B) were treated for 3.5 h with 10 ng/mL TNFα, 100 nM Smac-mimetic, and 10 μM IDN-6556 or for 6 h with 20 ng/mL TNFα, 100 nM Smac-mimetic, and 10 μM IDN-6556, respectively. Cell extracts were analyzed by western blotting.

Figure 14.

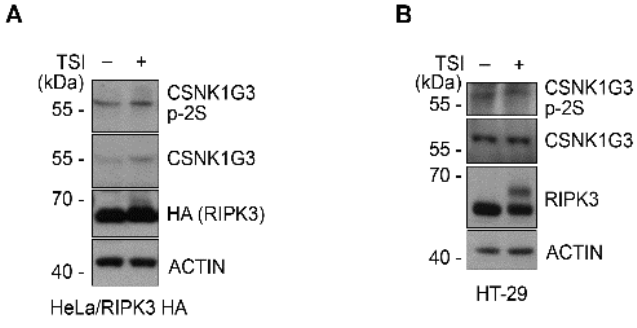
A
TSI – +
(kDa)
55 -
CSNK1G3 p-2S
55 -
CSNK1G3
70 -
HA (RIPK3)
40 -
ACTIN
HeLa/RIPK3 HA
B
TSI – +
(kDa)
55 -
CSNK1G3 p-2S
55 -
CSNK1G3
70 -
RIPK3
40 -
ACTIN
HT-29

Figure 15. Phosphorylated form of CK1γ3 at S344/345 is detected in the necrosome of SDS-soluble fraction. HeLa/RIPK3-HA were treated with TSI for 3 h and lyzed in 1% Triton X-100. Undissolved pellets were further lyzed with 1% SDS and finally diluted to 0.1% SDS (SDS-sup fraction) which was used in IP assay.

Figure 15.

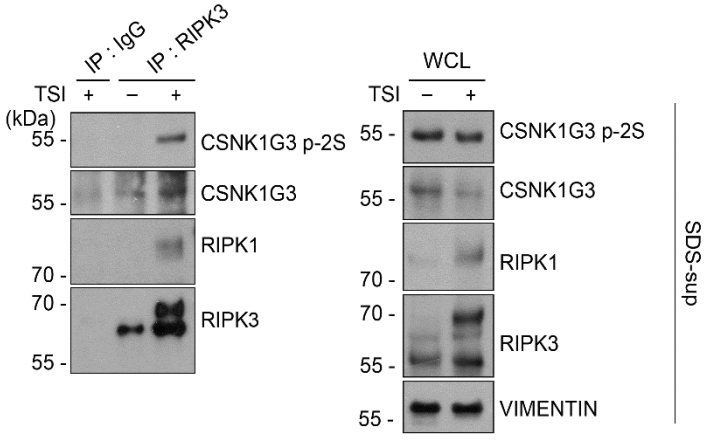
IP : IgG
IP : RIPK3
TSI + – +
(kDa)
55 -
CSNK1G3 p-2S
55 -
CSNK1G3
RIPK1
70 -
70 -
RIPK3
55 -
WCL
TSI – +
55 -
CSNK1G3 p-2S
55 -
CSNK1G3
RIPK1
70 -
70 -
RIPK3
55 -
55 -
VIMENTIN
SDS-sup

Figure 16. CK1γ inhibitor Gi protects mice against TNF-induced SIRS. (**A, B**)

Tail-vain injection of CK1γ inhibitor Gi protects mice form TNF-induced SIRS. Mice were injected with 3 mg/kg Gi or 7-Cl-O-Nec-1 (Nec1-s) through tail vein for 20 min before challenge by 20 μg mTNFα. Mouse survival rate (A) and body temperature (B) were measured every 2 h using a rectal thermometer probe.

Figure 16.

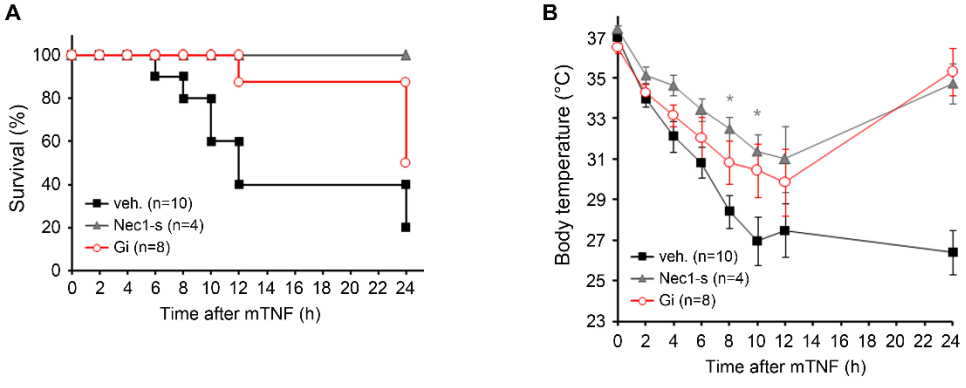
A
Survival (%)
100
80
60
40
20
0
0 2 4 6 8 10 12 14 16 18 20 22 24
Time after mTNF (h)
veh. (n=10)
Nec1-s (n=4)
Gi (n=8)
B
Body temperature (°C)
37
35
33
31
29
27
25
23
0 2 4 6 8 10 12 14 16 18 20 22 24
Time after mTNF (h)
veh. (n=10)
Nec1-s (n=4)
Gi (n=8)
*
*

Figure 17. A proposed model for the mechanism by which CK1γ contributes to necroptosis activation.

Figure 17.

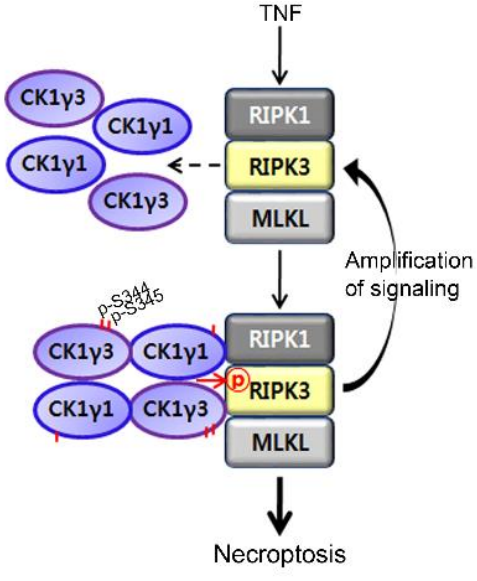
TNF
CK1γ3
CK1γ1
CK1γ1
CK1γ3
RIPK1
RIPK3
MLKL
Amplification
of signaling
p-S344
p-S345
CK1γ3
CK1γ1
CK1γ1
CK1γ3
RIPK1
P
RIPK3
MLKL
Necroptosis

Figure 18. The levels of CK1γ1 and CK1γ3 are regulated NAC during TSI-induced necroptosis. HeLa/RIPK3-HA cells were pretreated for 30 min with 5 mM N-acetyl-L-cystein (NAC) and then treated with TSI in the presence or absence of 10 μM Nec1 or 5 mM NAC.

Figure 18.

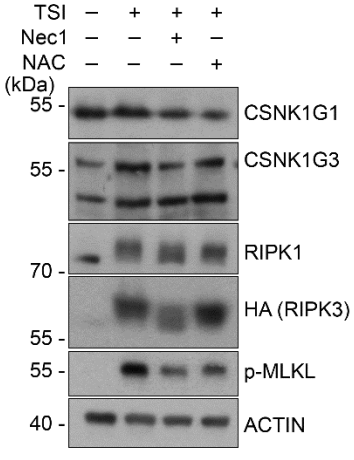
TSI – + + +
Nec1 – – + –
NAC – – – +
(kDa)
55 -
CSNK1G1
55 -
CSNK1G3
70 -
RIPK1
55 -
HA (RIPK3)
55 -
p-MLKL
40 -
ACTIN

Table 1. The number and ratio of phosphorylated peptides at S344 or S345 of CK1γ3 identified by liquid chromatography tandem-mass spectrometry (LC-MS/MS).

Site	Phospho-peptide
S344	QLPTPVGAVQQDPALS*SNREAHQHR
S345	QLPTPVGAVQQDPALSS*NREAHQHR

	The number of peptides identified phosphorylated:non-phosphorylated (ratio, %)	
Site	**NT**	**TSI**
S344	15:78 (16.13 %)	22:87 (20.18 %)
S345	9:84 (9.68 %)	15:94 (13.76 %)

4. DISCUSSION

During last a decade, a great advance in understanding necroptosis, a special type of necrosis, has been achieved by identifying RIPK family and its downstream MLKL. Considering apoptosis, however, there is no doubt in that other signals and factors, besides these molecules, also can regulate necroptosis and lots of efforts have thus been put into a research field to identify new regulators involved. To identify such regulators of necroptosis, I took an advantage of the gain-of-functional (GOF) screening utilizing cDNA expression library. Compared to the loss-of-functional (LOF) screening using siRNA library, GOF screening is advantageous over LOF screening to isolate novel factors in such a condition that the signal to activate them is not operating. In addition, given that CK1γ is a long-lived protein, it is hard to define its function through transient knockdown experiments in the LOF screening. Moreover, I now know that at least CK1γ3 could functionally complement CK1γ1, as shown in CK1γ1 knockout cells, showing that downregulation of one isoform rarely affects cell fate.

While CK1γ isoforms show a high homology in their primary protein sequences, they are located in different subcellular fractions and function in distinct ways in necroptosis. To define a role of CK1γ more precisely, I used a CK1γ-specific inhibitor Gi. Gi was reported to act more selectively toward CK1γs (CK1γ IC_{50} = 0.029 μM, CK1α IC_{50} = 7.58 μM, CK1δ IC_{50} = 2.62 μM) (Hua Z, et al., 2012). CK1γ is known to be palmitoylated at the C-terminus for the membrane localization (Davidson G, et al., 2005). Nevertheless, I found some distinct characteristics among CK1γs. First, CK1γ3 tends to locate in more insoluble parts of cells than CK1γ1 does, and CK1γ2 is found in the most soluble localization in cells. Unlike to RIPK1, RIPK3 and MLKL which move to insoluble fraction once activated, however, the subcellular localization of all CK1γ isoforms remain unchanged during necroptosis induction. Given that the active necrosomes exist in highly insoluble compartments in cells, this might be the reason why CK1γ3 most effectively affects necroptosis among CK1γ isoforms. In addition, CK1γ1 is clearly cleaved by caspase-8 during apoptosis, which might probably suppress necroptosis when caspase-8 remains active, as seen in RIPK1. Those

fragmented proteins did not appear I did the same experiments with CK1γ3, at least. Lastly, it is interesting to note that CK1γ1 and CK1γ3, but not CK1γ2, were accumulated in necroptotic cells. This evokes the results that among CK1γ isoforms, only CK1γ2 had no effect on increasing necroptosis when etopically expressed. In addition, exogenous CK1γ1 and CK1γ3 can form heterodimer and CK1γs are found in the insoluble subcellular compartments, although there remains a question about the endogenous CK1γ1 and CK1γ3 actually interact in cells. This raises a possibility that CK1γ1 and CK1γ3 have a potential to form oligomers, like MLKL (Wang H, et al., 2014), or higher-order protein complexes, as in RIPK1-RIPK3 amyloid-like structure (Li J, et al., 2012).

It remains unclear how CK1γ is activated upon necroptosis. To date, the roles of reactive oxygen species (ROS) in necroptosis have been known to be somewhat confusing (Blaser H, et al., 2016). ROS, especially those generated in the mitochondria, have long been considered to have a significant effect on necroptosis (Schulze-Osthoff K, et al., 1992; Cho, YS, et al., 2009; Zhang, D.W. et al., 2009; Vanlangenakker N, et al., 2011), though, they do not participate in

necroptosis of all types of cells when their impacts examined with the antioxidants (He S, et al., 2009). Recently, RIPK3 was reported to mediate the production of necroptosis-induced ROS by promoting mitochondrial aerobic respiration via pyruvate dehydrogenase complex (PDC) activation (Yang Z, et al., 2018). In case of RIPK1, cysteine residues in the protein were shown to be oxidized by ROS produced during necroptosis and form disulfide bonds, resulting in formation of high molecular weight RIPK1 complex. And this oxidization may be important for the autophosphorylation of RIPK1 on Ser-161 and thus for its activation (Zhang Y, et al., 2017). Likewise, I observed that overexpressed CK1γ was autophosphorylated, as reported (Zhai L, et al., 1995) and kinase dead mutants of CK1γ1 and CK1γ3 do not have pro-necroptotic activity. The above results lead me to guess that CK1γ activation is also influenced by ROS produced in necroptotic cells. Accordingly, I also found that CK1γ level was regulated by ROS during necroptosis (Fig. 18). To date, the roles of ROS in necroptosis have been known to be somewhat confusing. However, it should be confirmed further whether the increased levels of CK1γ directly affect its activity.

After CK1γ is activated in parallel with RIPK1, RIPK3 and MLKL, it is very interestingly to note that CK1γ phosphorylates RIPK3, not *vice versa*. The crucial question to be answered is whether the phosphorylation of RIPK3 by CK1γ means the activation of RIPK3. I observed the reduction in the phosphorylation of MLKL Ser358 in Gi-treated or CK1γ knockout cells, and consequentially the impairment in the formation of MLKL oligomers. Because MLKL Ser358 is known to be phosphorylated by active RIPK3, I believe that CK1γ may be engaged in RIPK3 activation. Given that decrease of phospho-MLKL level was not as much significant as decline in cell death rate by CK1γ inhibition (either by an inhibitor or knockout of genes), however, the aforementioned result is likely a consequence of the failure in producing a positive feedback loop in CK1γ-inhibited cell. Supposing that is the case, the other chance that CK1γ regulates necroptosis via RIPK3 activation might lie on steps at (i) phosphorylation on MLKL other than the previously known residues, such as Thr357 and Ser358 in human MLKL, (ii) translocation of MLKL to plasma membrane or (iii) other factors activated by MLKL in the cell membrane. Some of MLKL mutants that can form oligomers

and translocate to plasma membrane but cannot kill cells have been reported (Wang H, et al., 2014). Membrane translocation of MLKL alone is not generally accepted to be sufficient for causing necroptosis. And up to date, TRPM7, a cation channel located in plasma membrane, is the only known mediator downstream of RIPK3/MLKL (Cai Z, et al., 2013). It cannot be excluded that CK1γ could help TRPM7 or not yet uncovered elements to be activated.

In conclusion, it is evident that CK1γs, especially CK1γ1 and CK1γ3, are essential mediators in TNFα-induced necroptosis (Fig. 17). Activated by necroptotic stimuli, CK1γ forms a protein complex with the necrosome and phosphorylates RIPK3 for further activation of necroptosis (Fig. 17).

5. REFERENCES

Blaser H, et al. (2016) TNF and ROS Crosstalk in Inflammation. Trends in Cell Biol 26:249–261.

Cai Z, et al. (2013) Plasma membrane translocation of trimerized MLKL protein is required for TNF-induced necroptosis. Nat Cell Biol 16:55-65.

Chen W, et al. (2013) Diverse Sequence Determinants Control Human and Mouse Receptor Interacting Protein 3 (RIP3) and Mixed Lineage Kinase domain-Like (MLKL) Interaction in Necroptotic Signaling. J Biol Chem 288:16247–16261.

Chen W, et al. (2015) Ppm1b negatively regulates necroptosis through dephosphorylating Rip3. Nat Cell Biol 17:434-444.

Cheong J, Virshup D (2011) Casein kinase 1: Complexity in the family. Int J

Biochem Cell Biol 43:465-469.

Cho, YS, et al. (2009) Phosphorylation-driven assembly of the RIP1–RIP3 complex regulates programmed necrosis and virus-induced inflammation. Cell 137:1112–1123.

Christofferson DE, Yuan J (2010) Necroptosis as an alternative form of programmed cell death. Curr Opin Cell Biol 22:263–268.

Davidson G, et al. (2005) Casein kinase 1 gamma couples Wnt receptor activation to cytoplasmic signal transduction. Nature 438:867-872.

Declercq W, et al. (2009) RIP Kinases at the Crossroads of Cell Death and Survival. Cell 138: 229-232.

Degterev A, et al. (2005) Chemical inhibitor of nonapoptotic cell death with

therapeutic potential for ischemic brain injury. Nat Chem Biol 1:112–119.

Degterev A, et al. (2008) Identification of RIP1 kinase as a specific cellular target of necrostatins. Nat Chem Biol 4:313–321.

Degterev A, et al. (2013) Activity and specificity of necrostatin-1, small-molecule inhibitor of RIP1 kinase. Cell Death Differ 20:366.

Dillon CP, et al. (2014) RIPK1 blocks early postnatal lethality mediated by caspase-8 and RIPK3. Cell 157:1189–1202.

Dondelinger Y, et al. (2017) MK2 phosphorylation of RIPK1 regulates TNF-mediated cell death. Nat Cell Biol 19:1237–1247.

Duprez L, et al. (2011) RIP kinase-dependent necrosis drives lethal systemic inflammatory response syndrome. Immunity 35:908–918.

Feng S, et al. (2007) Cleavage of RIP3 inactivates its caspase-independent apoptosis pathway by removal of kinase domain. Cell Signal 19:2056-2067.

Geng J, et al. (2017) Regulation of RIPK1 activation by TAK1-mediated phosphorylation dictates apoptosis and necroptosis. Nat Commun 8:359.

He S, et al. (2009) Receptor interacting protein kinase-3 determines cellular necrotic response to TNF-α. Cell 137:1100–1111.

Hua Z, et al. (2012) 2-Phenylamino-6-cyano-1H-benzimidazole-based isoform selective casein kinase 1 gamma (CK1γ) inhibitors. Bioorg Med Chem Lett 22:5392-5395.

Jaco I, et al. (2017) MK2 phosphorylates RIPK1 to prevent TNF-induced cell death. Mol Cell 66:698–710 e695.

Kaiser WJ, et al. (2011) RIP3 mediates the embryonic lethality of caspase-8-deficient mice. Nature 471:368–372.

Li J, et al. (2012) The RIP1/RIP3 necrosome forms a functional amyloid signaling complex required for programmed necrosis. Cell 150:339–350.

Lin Y, et al. (1999) Cleavage of the death domain kinase RIP by Caspase-8 prompts TNF-induced apoptosis. Genes Dev 13:2514–2526.

Linkermann A, et al. (2013) Two independent pathways of regulated necrosis mediate ischemia–reperfusion injury. Proc Natl Acad Sci USA. 110:12024-12029.

Liu X, et al. (2016) Post-translational modifications as key regulators of TNF-induced necroptosis. Cell Death Dis 7:e2293.

Murphy J, Vince J (2015) Post-translational control of RIPK3 and MLKL mediated necroptotic cell death. F1000Res :4:F1000 Faculty Rev-1297.

Murphy M, Silke J (2014) Ars Moriendi; the art of dying well – new insights into the molecular pathways of necroptotic cell death. EMBO Rep 15:155–164.

Newton K, et al. (2014) Activity of protein kinase RIPK3 determines whether cells die by necroptosis or apoptosis. Science 343:1357–1360.

Oberst A, et al. (2011) Catalytic activity of the caspase-8-FLIPL complex inhibits RIPK3-dependent necrosis. Nature 471:363–367.

Ofengeim D, et al. (2015) Activation of necroptosis in multiple sclerosis. Cell Rep 10:1836–1849.

Onizawa M, et al. (2015) The ubiquitin-modifying enzyme A20 restricts ubiquitination of the kinase RIPK3 and protects cells from necroptosis. Nat Immunol 16:618–627.

Rena G, et al. (2004) D4476, a cell-permeant inhibitor of CK1, suppresses the site-specific phosphorylation and nuclear exclusion of FOXO1a. EMBO Rep 5:60-65.

Rodriguez DA, et al. (2016) Characterization of RIPK3-mediated phosphorylation of the activation loop of MLKL during necroptosis. Cell Death Differ. 23:76–88.

Schittek B, Sinnberg T (2014) Biological functions of casein kinase 1 isoforms and putative roles in tumorigenesis. Mol Cancer 13:231.

Schulze-Osthoff K, et al. (1992) Cytotoxic activity of tumor necrosis factor

is mediated by early damage of mitochondrial functions. Evidence for the involvement of mitochondrial radical generation. J Biol Chem 15:5317-5323.

Shan B, et al. (2018) Necroptosis in development and diseases. Genes Dev 32:327-340.

Sun L, et al. (2012) Mixed lineage kinase domain-like protein mediates necrosis signaling downstream of RIP3 kinase. Cell 148:213–227.

Vanlangenakker N, et al. (2011) TNF-induced necroptosis in L929 cells is tightly regulated by multiple TNFR1 complex I and II members. Cell Death Dis 2:e230.

Wang H, et al. (2014) Mixed lineage kinase domain-like protein MLKL causes necrotic membrane disruption upon phosphorylation by RIP3. Mol Cell 54:133–146.

Wang X, et al. (2008) TNF-alpha induces two distinct caspase-8 activation pathways. Cell 133:693-703.

Wang Z, et al. (2012) The mitochondrial phosphatase PGAM5 functions at the convergence point of multiple necrotic death pathways. Cell 148:228-243.

Wertz IE, et al. (2004) De-ubiquitination and ubiquitin ligase domains of A20 downregulate NF-kappaB signalling. Nature 430:694–699.

Yang Z, et al. (2018) RIP3 targets pyruvate dehydrogenase complex to increase aerobic respiration in TNF-induced necroptosis. Nat Cell Biol 20:186–197.

Zhai L, et al. (1995) Casein Kinase Iγ Subfamily. J Biol Chem 270:12717-12724.

Zhang, DW. et al. (2009) RIP3, an energy metabolism regulator that switches TNF-induced cell death from apoptosis to necrosis. Science 325:332–336.

Zhang H, et al. (2011) Functional complementation between FADD and RIP1 in embryos and lymphocytes. Nature 471:373–376.

Zhang Y, et al. (2017) RIP1 autophosphorylation is promoted by mitochondrial ROS and is essential for RIP3 recruitment into necrosome. Nat Commun 8:14329.

6. 국문초록

세포괴사 (necroptosis) 과정은 caspase의 활성이 저해되었을 때, 대안적 세포죽음 기작으로써 배아 발달뿐만 아니라 바이러스 및 박테리아 감염, 염증 반응, 퇴행성 뇌질환 등 여러 병리학적 상황에서의 역할이 점차 주목받고 있다. 이 과정에서 단백질 키나아제 RIPK1, RIPK3의 활성 및 이들이 키나아제 유사체 MLKL과 함께 복합체 (necrosome) 를 형성하는 것이 세포 죽음을 일으키는 데 중요하다고 알려져 있으나 이 외 다른 단백질의 기능에 대해서는 거의 알려져 있지 않다.

본 연구에서는 RIPK1, RIPK3와 더불어 세포괴사를 조절할 수 있는 또 다른 인자를 찾기 위해 650 개의 키나아제와 120 개의 포스파타아제 cDNA 를 이용하며 스크리닝을 진행하였으며, 카세인 키나아제 1 감마 (CK1γ) 가 세포괴사를 증진시키는 것으로 확인되었다. CK1γ1과 CK1γ3의 knockout 및 화학적 억제제를

사용한 CK1γ 활성 억제 결과, TNFα에 의해 유발되는 세포괴사가 감소하는 결과를 보였으나, CK1γ 과발현이 세포사멸 (apoptosis)에는 영향을 끼치지 않았다.

또한 CK1γ1은 RIPK1과 RIPK3와 마찬가지로, 세포가 세포사멸을 겪는 동안 caspase-8에 의해 절단된다. 이와 반대로 세포괴사 과정에서 CK1γ1과 CK1γ3는 그 양이 증가하는데, CK1γ1 또는 CK1γ3의 과별현이 세포괴사를 증가시켰던 것과는 다르게 CK1γ2의 과별현은 세포괴사에 영향이 없었던 것과 유사하게 세포괴사를 겪는 세포에서 CK1γ2의 증가도 확인 할 수 없었다. CK1γ1 과 CK1γ3 가 세포괴사 과정에서 어떻게 기여하는지 알아보기 위해 면역침강 실험을 진행하였고 RIPK1, RIPK3, MLKL 등 세포괴사 단백질 복합체와 결합하는 것이 확인되었다. 특히 CK1γ3 경우, 344/345 번째 세린에 자가인산화된 형태가 세포괴사 복합체에서 검출되었고 이 세린이

알라닌으로 치환되었을 때는 CK1γ3 과발현이 세포괴사를 일으키는 능력이 현저히 떨어지는 것이 발견되었다. 또한 CK1γ는 *in vitro* 에서 RIPK3를 인산화시키고, CK1γ 특이적 억제제 Gi는 RIPK3의 타깃 사이트로 알려진 MLKL Ser358의 인산화뿐 아니라 MLKL 올리고머 형성을 감소시켰다. 더불어 Gi 는 TNFα에 의해 유발 된 전신성 염증 반응 증후군 (SIRS) 으로부터 마우스를 보호하였다. 종합적으로, 위 실험 결과는 CK1γ1 및 CK1γ3이 RIPK3 인산화를 통한 세포괴사 복합체의 형성을 조절함으로써 세포괴사 진행을 촉진 시키는데 필요하다는 것을 보여준다.